



Cite this: *RSC Sustainability*, 2026, **4**, 896

## Mixture design of experiments to improve fungal degradation of cosmetic pigments

Erika Ribezzi,<sup>a</sup> Fabio Fornari,<sup>a</sup> Nicolo' Riboni,<sup>†\*ab</sup> Maria Vittoria Rizzo,<sup>bc</sup> Monica Mattarozzi,<sup>a</sup> Maurizio Piergiovanni,<sup>a</sup> Alessandra Mori,<sup>d</sup> Paolo Goi,<sup>d</sup> Corrado Sciancalepore,<sup>bc</sup> Daniel Milanese,<sup>bc</sup> Giuseppe Vignali,<sup>bc</sup> Federica Bianchi,<sup>†\*ab</sup> and Maria Careri<sup>a</sup>

In response to the increasing demand for sustainable waste management and circular economy strategies, this study explores the bioremediation of cosmetic waste—specifically permanent oxidative hair dyes—using white-rot fungi and the subsequent valorisation into fungal-based biocomposite materials. Three fungal species (*Trametes versicolor*, *Pleurotus ostreatus*, and *Ganoderma lucidum*) were evaluated for their ability to degrade two model dye systems, each composed of a primary dye and a coupler. For the first time, a mixture design of experiments was applied to optimize fungal growth on substrates made from industrial cardboard waste and dye formulations, achieving 60% incorporation of waste-derived components. A quick, easy, cheap, effective, rugged, and safe extraction method coupled with ultra-high performance liquid chromatography-diode array detection enabled accurate quantification of dye degradation. Method validation confirmed low detection limits (2.2–5.6 mg kg<sup>-1</sup>), high extraction recoveries ( $\geq 83\%$ ), and negligible matrix effect. Under optimized conditions, over 99% degradation of most dyes was achieved within 7 days. The environmental sustainability of the entire process was evaluated through Life Cycle Assessment (LCA) using the Environmental Footprint 3.1 method. Among 16 impact categories, machinery energy consumption generated the greatest impact, when compared to materials, their transportation and laboratory equipment.

Received 30th September 2025  
Accepted 17th December 2025

DOI: 10.1039/d5su00770d  
[rsc.li/rscsus](http://rsc.li/rscsus)

### Sustainability spotlight

This study addresses sustainable solutions in waste management and circular economy investigating the degradation of cosmetic waste using white-rot fungi. A novel aspect of this study is the use of a mixture design of experiments to optimize fungal growth on substrates made from industrial cardboard and dye residues, increasing waste-derived content from 37% to 60%. This was confirmed via eco-friendly QuEChERS extraction and UHPLC-DAD analysis. A gate-to-gate LCA revealed machinery energy use as the main environmental hotspot. The resulting biodegradable fungal-based biocomposites are intended for future use as compostable secondary packaging. Aligned with the UN Sustainable Development Goal Responsible Consumption and Production, this work promotes circular economy and green chemistry by turning industrial waste into valuable, low-impact materials.

## 1 Introduction

In recent years, the circular economy has emerged as a fundamental principle in both industrial and environmental policy on a global scale, prompting a shift from the traditional linear

manufacturing model to a more circular, sustainable approach.<sup>1</sup> In this context, the development of effective strategies and sustainable approaches to waste management and low-carbon footprint processes is demanded.

The ingredients in cosmetic formulations, including hair dyes, are classified as Personal Care Products<sup>2,3</sup> and are recognized as emerging contaminants. Permanent oxidative hair dyes, the most widely used on the market, lack inherent pigmentation and through chemical reactions form colored compounds that absorb light in the 380–780 nm range. Depending on their role in the chemical reaction, the molecules involved in the formation of such colored compounds can be classified into two groups: primary dyes and couplers. Primary dyes, typically aniline derivatives, are susceptible to oxidation, which converts them into reactive intermediates. Subsequently, the coupling dyes react with the reactive intermediates to form

<sup>a</sup>University of Parma, Department of Chemistry, Life Science and Environmental Sustainability, Parco Area delle Scienze 17/A, Parma, 43124, Italy. E-mail: [nicolo.riboni@unipr.it](mailto:nicolo.riboni@unipr.it); Tel: +390521902174

<sup>b</sup>University of Parma, CIPACK (Interdepartmental Center for the Packaging), Parco Area delle Scienze 181/A, Parma, 43124, Italy. E-mail: [federica.bianchi@unipr.it](mailto:federica.bianchi@unipr.it); Tel: +390521905446

<sup>c</sup>University of Parma, Department of Systems Engineering and Industrial Technologies, Parco Area delle Scienze 181/A, Parma, 43124, Italy

<sup>d</sup>Davines SpA, Via Calzolari Don Angelo 55a, Parma, 43126, Italy

† Present address: Customs and Monopolies Agency, Local Directorate of Lombardy, Via Marco Bruto 14, Milan, 20138, Italy.



the final dye molecules.<sup>4,5</sup> Due to their hazardous nature, many of these compounds have been banned<sup>6</sup> or are subjected to restricted use.<sup>7</sup> Consequently, improper disposal of hair dye residues represents a significant environmental concern, as these substances have the potential to act as hazardous pollutants.

White-rot fungi (WRFs) are renowned for their ability to entirely degrade lignin through the secretion of a pool of highly specialized exoenzymes.<sup>8,9</sup> In this context, laccases are of particular interest, due to their wide range of potential biotechnological applications, including the degradation of pollutants.<sup>10,11</sup> Evidence suggests the effectiveness of fungal and bacterial laccases in degrading organic dyes through oxidative reactions, establishing the basis for the utilization of laccase-producing organisms in waste bioremediation.<sup>12–14</sup> Finally, mycelium-based composites can offer a cost-effective, renewable, recyclable and biodegradable alternative to traditional packaging.<sup>15,16</sup>

To assess the effectiveness of dye degradation, proper sample clean-up and extraction protocols are required. According to the principles of green analytical chemistry, quick, easy, cheap, effective, robust (QuEChERS)-based methods have been proposed as green and user-friendly alternatives to traditional extraction techniques.<sup>17,18</sup> This extraction technique relies on a low-cost two-step sample preparation approach consisting of a salting-out extraction, followed by a clean-up step based on dispersive solid-phase extraction.

The aim of the study was to evaluate the degradation capability of three fungal species against permanent oxidative dyes, with the goal of providing a sustainable approach for waste management. A mycelium-based material deriving from dye degradation that could be used as secondary packaging was also forecasted. This strategy enables the integration of bioremediation and biocomposite production in a unique approach. For the first time, a chemometric approach based on a mixture design of experiments was proposed as a valuable tool to optimize the culture conditions for *in vitro* fungal growth. Then, a QuEChERS-ultra-high performance liquid chromatography-diode array detection (UHPLC-DAD) method was developed and validated to evaluate the degradation efficiency toward both primary dyes and their couplers. Finally, a gate-to-gate Life Cycle Assessment (LCA) conducted at laboratory scale was carried out to evaluate the environmental sustainability of the entire process.

## 2 Experimental

### 2.1 Optimization of fungal growth conditions

The effect of culture medium composition on fungal growth was investigated using dye formulations without pigments as blank matrix. A mixture design of experiments was applied to study the effect of three factors: the amount of cardboard, dye, and mycelium. The experiments were designed in the pseudo-component domain ( $X_1$ ,  $X_2$ , and  $X_3$ ) as described in SI and Table S1. For each fungal species, a total of  $N = 15$  experiments were carried out in random order (Table S2), including  $n_0 = 3$  experiments at the center of the experimental domain to

estimate the pure experimental variance. The wavelengths used are reported in Table S3.

Three response variables were defined as follows: (i) germination time ( $t_G$ ), *i.e.* the amount in time (in hours) elapsed until visible growth was observed; (ii) shape factor ( $S_f$ ), a qualitative measure reflecting the ease of mixing and the ability of the culture to retain its shape upon removal of the capsules after thermal treatment (the evaluation was performed using a six-point scale 1–6); (iii) the mixture factor, corresponding to the amount of dye ( $m_d$ , expressed in g) used in the formulation of the growth medium. The model regression is reported in SI.

Cultures were prepared under the optimized fungal growth conditions, namely 2.96 g of cardboard, 3.81 g of mycelium, 2.73 g of dye and 10 mL of a 2.05% v/v aqueous lactic acid solution. Two pigment combinations were tested as model compounds, *i.e.*, toluene-2,5-diamine sulfate (PTD) + 2-methylresorcinol (2MR), and *p*-aminophenol (PAP) + 4-amino-2-hydroxytoluene (PAOC). The experiments were planned according to a two-way analysis of variance (ANOVA) without replicates as described in SI.

### 2.2 QuEChERS extraction

The QuEChERS extraction procedure was carried out by selecting the most suitable extraction salts (factor A, see SI) for salting-out partitioning and evaluating the most effective dSPE sorbent (factor B, see SI) for sample clean-up, with the aim of maximizing the recovery of the organic dyes from the culture medium.

### 2.3 Degradation experiments

Cultures were prepared according to the optimized fungal growth conditions evaluating 3 different incubation times: 0, 4 and 7 days. Three replicate measurements were obtained for each incubation time. Control samples, prepared in the absence of mycelium, were also included. Details are reported in SI.

### 2.4 Method validation

The UHPLC-DAD method was validated under the optimised conditions according to the EURACHEM guidelines.<sup>19</sup> Limits of detection (LODs) and limits of quantitation (LOQs), linearity, precision, trueness and selectivity were assessed. A detailed description is provided in SI.

### 2.5 Life cycle assessment

To analyze the environmental impact of the substrate production process, the Life Cycle Assessment approach was used. In the analysis of the laboratory-scale process, a “gate to gate” approach was considered, according to the ISO 14040 (Environmental management, Life cycle assessment, Principles and framework) and ISO 14044 (Life Cycle Assessment, Requirements and Guidelines) standard guidelines.<sup>20,21</sup> The analysis followed the LCA structure suggested by the ISO: (1) goal and scope definition, (2) life cycle inventory (LCI), (3) life cycle impact assessment (LCIA) and (4) interpretation of the results.



The software SimaPro 10.1 including the Ecoinvent version 3.10 database was used. Details of each LCA step are reported in SI.

## 2.6 Development and characterization of bio-composite materials

After seven days of incubation, the cultures were heat-treated at 120 °C for nine hours. The material was subsequently ground several times using a planetary mill to reduce the powder granulometry down to 50 µm. Mixtures of polybutylene adipate terephthalate (PBAT) as polymer matrix and the fungal substrate as filler were prepared at different concentrations (10–20–30% w/w). Pure PBAT was used as reference. After extrusion and injection molding, the dumbbell specimens were used for the mechanical characterization of the various composite formulations. The Young's modulus, the yield stress, and the ultimate tensile stress were obtained from the stress-strain curves. More precisely, Young's modulus, which is calculated as the slope of the straight section of the curve, defines the stiffness of the material, *i.e.* its tendency to plastic deformation when subjected to a load; the maximum of the curve following the straight section corresponds to the irreversible plastic behavior of the material, otherwise known as the yield stress and the maximum stress, also defined as ultimate tensile stress, is the stress required to break the specimen.

## 3 Results and discussion

### 3.1 Mixture design for the optimization of fungal growth conditions

A mixture design of experiments is proposed as a valuable strategy to enhance the growth of various fungal species for the bioremediation of cosmetic wastes. White-rot fungi (WRF) were selected due to their excellent adaptability to environmental challenges. Furthermore, they have shown promising results in the decolorization of dyes and bioremediation of organic pollutants.<sup>22,23</sup> Among WRF, *Trametes versicolor* (TV), *Pleurotus ostreatus* (PO) and *Ganoderma lucidum* (GL) were selected since they are known to produce highly effective ligninolytic enzyme systems able to promote the breakdown of diverse synthetic dyes. These enzymes mainly belong to laccases, manganese peroxidase, dye-decolorizing peroxidases, and lignin peroxidase. Laccases catalyze the reduction of oxygen to water while simultaneously oxidizing a broad range of substrates, primarily phenolic compounds.<sup>24</sup> Manganese peroxidases are heme-containing glycoproteins belonging to the oxidoreductase group that can catalyze the degradation of toxic dye pollutants, phenolic compounds, antibiotics, and other hazardous environmental contaminants.<sup>25</sup> Dye-decolorizing peroxidase enzymes are present in both fungi and bacterial, playing a key role the degradation of lignin and anthraquinones.<sup>26</sup> Finally, lignin peroxidase was applied for the decolorization of synthetic textile dyes.<sup>27</sup> TV is one of the most studied species, owing to its ability to tolerate non-sterile conditions, which makes it easier to handle and cultivate even for non-specialists. It produces high levels of extracellular oxidative enzymes, including high-redox-potential laccases, manganese peroxidase, and lignin

peroxidase.<sup>28</sup> In addition, it has been widely suggested for the decolorization of dyes.<sup>23</sup> PO is characterized by the absence of lignin peroxidases and the presence of three versatile peroxidases and six manganese peroxidases: genomic analysis revealed that versatile peroxides exert the role typical of lignin peroxides.<sup>29</sup> In addition, the production of dye decolorizing peroxidases has been recently investigated.<sup>30</sup> PO has been also applied for bioremediation purposes.<sup>31,32</sup> Finally, GL produces several highly stable laccase isoenzymes, frequently tolerant to fluctuations in pH and temperature,<sup>33</sup> which is advantageous for the bioremediation of dyes.<sup>34</sup>

After performing the experiments, multiple linear regression was carried out to calculate the models.<sup>35</sup> All the models were validated in terms of goodness-of-fit (ANOVA,  $p > 0.01$ ), indicating that the approximation error could be explained in terms of experimental variance. Regarding germination time, the models (Table 1) demonstrated good performance in terms of both explained variance and predictive capability in cross-validation, with  $R^2 \geq 0.98$  and  $Q^2 \geq 0.86$ , respectively – the latter being exceptionally good considering the biological nature of the process. Fig. S1 and S2 depict the ternary contour plots.

All fungal species exhibited similar behavior. The terms related to pseudo-components  $X_1$  and  $X_2$  as well as the interaction term between  $X_2$  and  $X_3$  resulted to be significant in all models. By contrast, the term related to pseudo-component  $X_3$  appeared only in the model related to TV. The effect associated with pseudo-component  $X_2$  showed the highest magnitude among all terms, as the largest variation in response was observed when comparing  $t_G$  at 100%  $X_2$  to that at 50%  $X_1$  and 50%  $X_3$ . Conversely, the effect related to  $X_1$  was the weakest.

For all species, visible growth was observed only after prolonged incubation when higher proportions of pseudo-component  $X_2$  (rich in hair dye) were present in the medium. By contrast, faster growth occurred with higher contents of pseudo-component  $X_3$  (rich in cardboard). Although these findings seem to contradict the commonly observed positive correlation between high nitrogen content and biomass production,<sup>36</sup> the observed behavior may be explained by the texture of the culture medium. In fact, higher proportions of  $X_2$

**Table 1** Regression models calculated for each species with respect to germination time, shape factor and amount of dye

	Models <sup>a</sup>
$t_G$	
TV	$y = 19(\pm 3)X_1 + 68(\pm 3)X_2 + 20(\pm 3)X_3 - 70(\pm 20)X_2X_3$
PO	$y = 40(\pm 10)X_1 + 160(\pm 10)X_2 - 190(\pm 60)X_2X_3$
GL	$y = 50(\pm 20)X_1 + 180(\pm 20)X_2 - 200(\pm 80)X_2X_3$
$S_f$	
TV	$y = 5(\pm 1)X_1$
PO	$y = 6(\pm 1)X_1 + 17(\pm 7)X_2X_3$
GL	$y = 4(\pm 1)X_1$
$m_d$ <sup>b</sup>	$y = 0.9X_1 + 4.7X_2 + 0.9X_3$

<sup>a</sup> The coefficients are reported as coefficient ( $\pm$  standard error) rounded at one significant digit. <sup>b</sup> The response corresponds to one of the mixture factors, the equation of the model is known.



led to a more liquid and compact consistency, whereas higher contents of  $X_3$  led to a drier and more porous structure. The latter condition allows for better air circulation compared to the more liquid texture, which could create an anoxic environment incompatible with fungal proliferation. As a general remark, TV was more tolerant than PO and GL with respect to the composition of the culture medium, as it showed visible growth in shorter times.

Conversely, GL exhibited the longest germination times across a wider portion of the pseudo-component domain. PO was characterized by an intermediate behavior (Fig. S1A).

As for the shape factor, the models (Table 1) showed good performance in terms of explained variance, while the predictive capability in cross-validation was acceptable, with  $R^2 \geq 0.93$  and  $Q^2 \geq 0.51$ . The ternary contour plots are depicted in Fig. S1B: the three species exhibited different behaviors regarding the ease of culture preparation and the texture of the resulting material after thermal treatment. The observed differences were most likely ascribable to the distinct textures of the mycelia themselves, both at the time of inoculation and after growth.

From the contour plots, it can be observed that the zones corresponding to the highest predicted values for  $S_f$  were located at low contents of pseudo-components  $X_2$  and  $X_3$ . Although cultures with higher proportions of pseudo-component  $X_2$  (rich in hair dye) were easier to homogenize, they lacked cohesion after thermal treatment. This behavior can be attributed to the limited fungal growth observed under these conditions, and from a full circularity perspective, hindered the recovery of the produced material for alternative uses, such as secondary packaging production. In contrast, cultures prepared with higher proportions of pseudo-component  $X_3$  (rich in cardboard) appeared drier and were difficult to homogenize. This could result in weak points in the final material and a deterioration of its mechanical properties. The best performance was observed at higher proportions of pseudo-component  $X_1$  (rich in mycelium), which consistently showed statistically significant effects. Combinations that promoted rapid fungal growth yielded samples that did not crumble after thermal treatment and can be ascribed to the binding effect of the mycelium, as previously reported in the literature.<sup>8</sup>

As for the amount of dye used for culture preparation, since this variable corresponded to one of the mixture components, the model equation did not need to be postulated (Table 1). As expected, in Fig. S2, the amount of hair dye increases linearly with higher proportions of pseudo-component  $X_2$  (*i.e.*, the component richest in hair dye).

Finally, Derringer's method was applied to identify the growth conditions that ensured the best compromise among the investigated responses. A global desirability  $D = 0.79$  was obtained, which was considered satisfactory, especially considering that some of the optimization criteria had opposite directions. Single desirability values close to 1 were achieved for the  $t_G$  of all investigated species, while  $d_i$  values higher than 0.42 and equal to 0.47 were calculated for the  $S_f$  and  $m_d$  parameters, respectively (Table S4). Globally, satisfactory optimal conditions were identified and considered valid, as the lack-of-fit was not

statistically significant ( $p > 0.01$ ). As a final remark, it should be noted that the use of an experimental design approach led to a significant improvement in waste management. Specifically, the initial composition included 37% of materials deriving from waste, whereas the newly identified composition reached 60% (Table 2).

### 3.2 QuEChERS optimization

Due to the high complexity of the matrix under investigation, a sample preparation step was necessary. For this purpose, the QuEChERS extraction technique was investigated and its performance was assessed by varying the composition of the extraction salt mixtures and the adsorbent used for the dSPE clean-up.

Three validated variants were tested: an unbuffered (UB)<sup>37</sup> and two buffered methods, one with acetic buffer (AOAC method)<sup>38</sup> and one with citrate buffer (EN method).<sup>39</sup> Since higher backgrounds in the UV-vis spectra were observed when the EN and AOAC methods were used, the UB method was selected as the most promising extraction strategy. Different dSPE sorbents were tested to determine their efficiency in removing interfering compounds. More precisely, PSA can aid the removal of acidic interferences, C18 can enhance the removal of fats and nonpolar interferences, graphitized carbon black can exert a positive effect on the removal of planar pigments, whereas Z-Sep can play a pivotal role in removing polar interferences. Preliminary evaluations were carried out *via* UV-vis spectroscopy planning the experiments according to an unreplicated two-ways ANOVA, meaning that all the possible combinations salts/sorbents were explored. As shown in Fig. S3, both factors had a negligible effect on the extraction of the investigated dyes ( $p > 0.05$ ). Although no statistically significant differences were obtained among the dSPE sorbents tested, visual inspection of the blank samples indicated that the PSA/C18+MgSO<sub>4</sub> combination produced the least pigmented and opalescent extracts. Consequently, this combination was chosen as sorbent phase for dSPE clean-up.

### 3.3 Chromatographic separation and method validation

Considering that commercial hair dye formulations usually contain more than one precursor and coupling agent, a UHPLC-DAD method was developed and validated to evaluate the degradation capability of the fungal species towards the investigated dyes. Different stationary phases were tested to provide an effective separation of the precursors, the coupling agents,

**Table 2** Composition (as weight fractions) related to the optimal conditions, expressed in the pseudo-component domain. Columns 3–5 and the last row show the back-conversion into the explicit mixture factors

Pseudo-component	Optimum	Cardboard	Dye	Mycelium
$X_1$	0.00	0.00	0.00	0.00
$X_2$	0.47	0.05	0.23	0.19
$X_3$	0.53	0.26	0.05	0.21
$\Sigma$	1.00	0.31	0.28	0.40



and the corresponding coupling products. A hydrophobic phase with pentafluorophenyl-propyl modification provided a higher selectivity compared to classical C18 functionalization due to a separation principle based on four retention mechanisms, namely polar interactions (H bonds), dipole–dipole interactions,  $\pi$ – $\pi$  interactions and hydrophobic interactions.

LOD and LOQ values were obtained in the 2.2–19 mg kg<sup>−1</sup> range (Table S5). A good linearity over two orders of magnitude was assessed for all pigments: no lack-of-fit was observed. RR% in the 83(±1) – 111(±5) % range ( $n = 10$ ) were obtained by analyzing blank matrices spiked with the investigated pigments at three different concentration levels: LOQ, 160 mg kg<sup>−1</sup> and 2500 mg kg<sup>−1</sup>. These results demonstrated the good efficiency of the developed method in terms of extraction recovery (Fig. S4). Method precision was evaluated at three concentration levels, namely LOQ, 160 mg kg<sup>−1</sup> and 2500 mg kg<sup>−1</sup> for each analyte: good results were obtained both in terms of intra-day repeatability and intermediate precision with RSD <3 and <10% at the highest and lowest concentration levels, respectively. Finally, the slopes of the calibration curves obtained from standard solutions and matrix-matched samples were not significantly different. Regarding the ME values, matrix effect factors of 36, 33, and 20% were observed for 2MR, PAP, and

PTD, respectively, while a much lower value (1.7%) was calculated for PAOC, confirming the presence of a negligible matrix effect.<sup>40</sup>

### 3.4 Pigment degradation over time

The validated UHPLC-DAD method was applied to study the degradation of pigments over time using each fungus alone and their combination. Day 0 was selected as the reference point, representing the initial condition in which 100% of each pigment was present in the culture. As previously stated, day 4 corresponded to the optimal germination time, while day 7 allowed for further fungal growth.

As for the binary PAP/PAOC, when PAP was considered (Fig. 1A), no significant difference was observed between treated and control samples on day 0 (ANOVA,  $p > 0.05$ ). On day 4, significant differences appeared with TVPO, GL and PO being the most effective treatments. After 7 days, TVPO allowed for an almost complete degradation of both pigments, with a percentage of 99.1(±0.9) %. A similar behavior was observed for PAOC (Fig. 1B). Regarding the coupling product (Fig. S5), on day 0 no significant differences were observed between the fungal species and the control sample except for the mix (Fig. 1C). On day 4, a general increase in the responses related to both the fungal-treated cultures and the control was observed. This effect was particularly marked for control samples, while

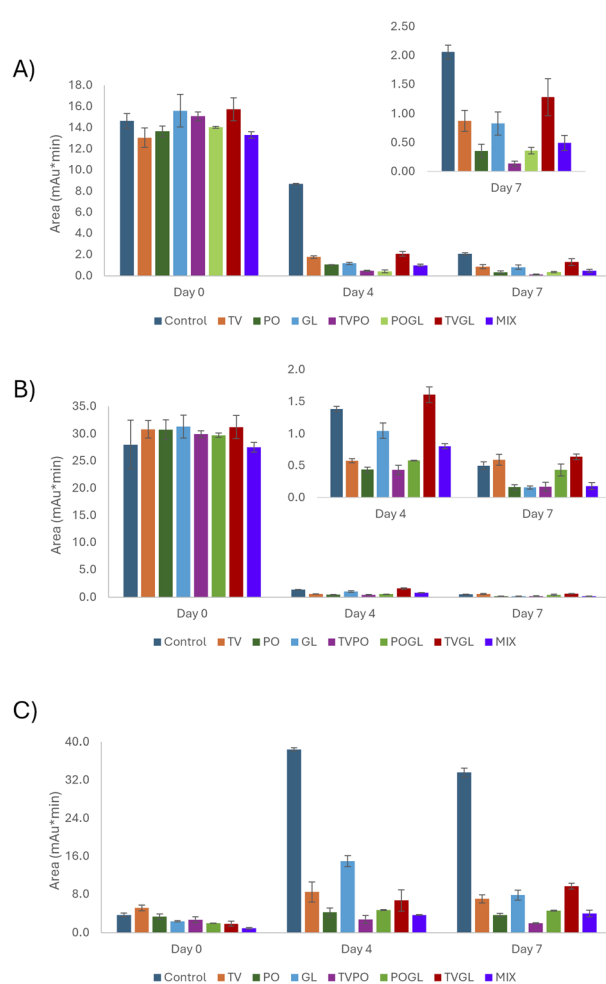


Fig. 1 Degradation of: (A) PAP; (B) PAOC; (C) coupling product.

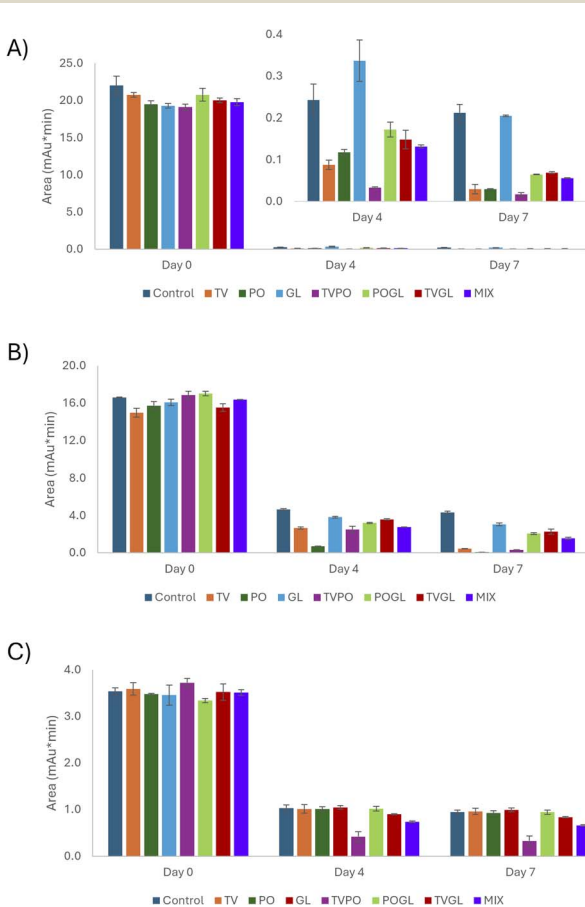


Fig. 2 Degradation of: (A) PTD; (B) 2 MR; (C) coupling product.



a reduced effect was evidenced for the fungal treatment. This behavior could be explained by considering the simultaneous combination of two effects: the formation of the coupling product and the degradation due to the enzymatic activity of the fungal species. The results obtained on day 7 were similar to those observed on day 4, with the exception of control and GL samples that showed a reduction in the observed responses.

Regarding the binary mixture PTD/2MR, for PTD (Fig. 2A) on day 0, no significant difference was observed among the responses. After four days, a strong decrease in the responses was observed for all samples, TV, PO and TVPO showing the highest degradation performance (>99%). A similar behavior was observed on day 7. 2MR (Fig. 2B) behaved similarly to PTD showing a significant decrease along the time, with a degradation in the 81–99.5% range for the fungal treatments. As for the coupling product (Fig. S5), a decrease in the responses was obtained between day 0 and day 4; no significant effect was observed for fungal treatments except for TVPO, which demonstrated the highest degradation capability (Fig. 2C).

### 3.5 Life cycle assessment

LCA was applied to quantify the environmental impacts associated with the laboratory-scale production of the innovative mycelium-based substrate and to identify the most challenging steps in the process. A gate-to-gate approach was adopted, encompassing substrate preparation, inoculation, and drying within the defined system boundaries. The results were then interpreted and discussed through Life Cycle Impact Assessment (LCIA). Fig. 3 shows the environmental impact profile of the mycelium-based substrate. The life cycle analyzed was divided into four main phases: (i) transport phases (transport of mycelium, lactic acid, cardboard, and hair dye); (ii) laboratory equipment (plastic tray, steel prop and spatula, ceramic capsule and pestle, parafilm, glass jar, tin cap deionized water and sterilizing agent); (iii) laboratory energy consumption (scale, autoclave, incubation, and heater); (iv) substrate material

### Sensitivity analysis on laboratory energy consumption

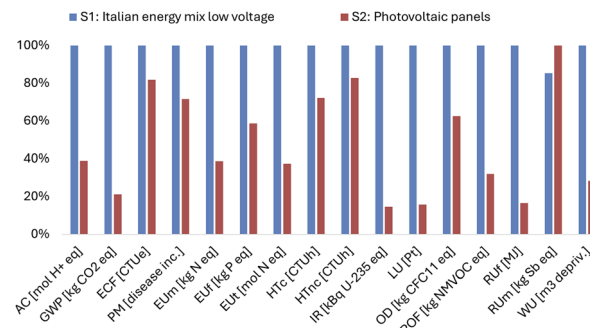


Fig. 4 Sensitivity analysis of the laboratory phase energy consumption.

composition (mycelium, cardboard, hair dye and lactic acid). The details are reported in SI, Table S6 and Fig. S6.

As shown in Fig. 3, the most impactful phase was the energy consumption of the machinery used during laboratory process. In particular, the incubation process was the most significant contributor in 14 out of 16 impact categories, with the exception of ECF (the harmful effects of toxic substances on biodiversity of freshwater ecosystems) and EUm (the excessive availability of a limiting nutrient that leads to the extent of the primary production in the ecosystem).<sup>41</sup> The incubation process is highly energy-consuming, as the equipment operates continuously for four days, resulting in a total energy consumption of 7.371 kWh per FU. The default Italian electricity mix from the Ecoinvent dataset “Electricity, low voltage {IT} | market for electricity, low voltage | Cut-off, S” was used to model all energy consumption. These findings are consistent with the results previously reported in the literature, where the equipment used on a laboratory scale is highly energy-intensive.<sup>42</sup> Within the same group, the second most impactful process was the heater used for final sample drying, operating for 2 hours and consuming 1.08 kWh per FU. These results are consistent with laboratory-scale production processes, particularly when small amounts of material are processed over extended periods. The contribution of hair dye was especially relevant for the impact categories ECF and EUm followed by HTc and OD. In addition, lactic acid production emerged as a significant contributor among the substrate materials, affecting the ECF, PM, EUm and POF categories.

Regarding the materials, the contribution of mycelium was notable in the EUm, LU and WU categories. In contrast, the transport ad materials equipment phases showed negligible impacts compared to the previously discussed contributions. The results of the life cycle impact assessment to produce the mycelium-based substrate are summarized in Table 3.

**3.5.1 Sensitivity analysis and industrial scale-up.** Since energy consumption for the processing stages has a significant impact, a sensitivity analysis was carried out, hypothesizing the use of a different energy source to assess the accuracy of the results. Sensitivity analysis consists of verifying how much the results change based on variations in the model or input data, in order to assess the robustness of the results (output data).<sup>43</sup>

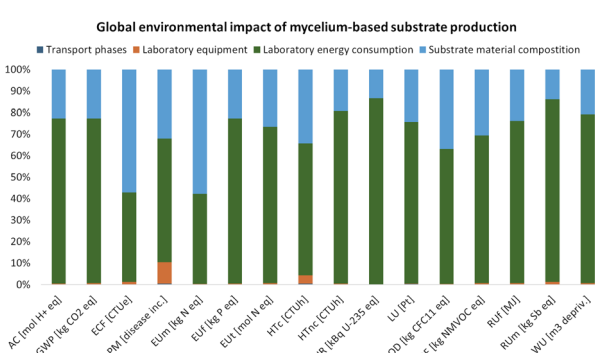


Fig. 3 Environmental impact of mycelium-based substrate production. Acidification (AC), climate change (GWP), ecotoxicity freshwater (ECF), particulate matter (PM), eutrophication marine (EUm), eutrophication freshwater (EUf), eutrophication terrestrial (EUT), human toxicity cancer (HTc), human toxicity non-cancer (HTnc), ionising radiation (IR), land use (LU), ozone depletion (OD), photchemical ozone formation (POF), resource use fossils (RUF), resource use minerals and metals (RUM) and water use (WU).



Table 3 Impact results of the mycelium-based substrate production according to the 16 E.F. 3.1 impacts categories

Impact category	Transport phases	Laboratory equipment	Laboratory energy consumption	Substrate material composition	Total
AC [mol H + eq]	$1.87 \times 10^{-5}$	$6.98 \times 10^{-5}$	$1.26 \times 10^{-2}$	$3.74 \times 10^{-3}$	$1.65 \times 10^{-2}$
GWP [kg CO <sub>2</sub> eq]	$8.97 \times 10^{-3}$	$1.80 \times 10^{-2}$	3.01	$8.97 \times 10^{-1}$	3.94
ECF [CTUE]	$3.43 \times 10^{-2}$	$2.13 \times 10^{-1}$	9.36	$1.28 \times 10^1$	$2.24 \times 10^1$
PM [disease inc.]	$6.60 \times 10^{-10}$	$1.05 \times 10^{-8}$	$6.24 \times 10^{-8}$	$3.47 \times 10^{-8}$	$1.08 \times 10^{-7}$
EUm [kg N eq]	$4.48 \times 10^{-6}$	$1.47 \times 10^{-5}$	$1.89 \times 10^{-3}$	$2.61 \times 10^{-3}$	$4.52 \times 10^{-3}$
EUf [kg P eq]	$6.07 \times 10^{-7}$	$4.72 \times 10^{-6}$	$6.70 \times 10^{-4}$	$1.98 \times 10^{-4}$	$8.73 \times 10^{-4}$
EUt [mol N eq]	$4.84 \times 10^{-5}$	$1.58 \times 10^{-4}$	$2.06 \times 10^{-2}$	$7.51 \times 10^{-3}$	$2.83 \times 10^{-2}$
HTc [CTUh]	$6.36 \times 10^{-11}$	$4.82 \times 10^{-10}$	$7.75 \times 10^{-9}$	$4.34 \times 10^{-9}$	$1.26 \times 10^{-8}$
HTnc [CTUh]	$7.92 \times 10^{-11}$	$1.79 \times 10^{-10}$	$3.74 \times 10^{-8}$	$8.95 \times 10^{-9}$	$4.66 \times 10^{-8}$
IR [kBq U-235 eq]	$1.64 \times 10^{-4}$	$7.90 \times 10^{-4}$	$3.58 \times 10^{-1}$	$5.57 \times 10^{-2}$	$4.15 \times 10^{-1}$
LU [Pt]	$7.62 \times 10^{-2}$	$6.53 \times 10^{-2}$	$1.76 \times 10^1$	5.71	$2.34 \times 10^1$
OD [kg CFC11 eq]	$1.78 \times 10^{-10}$	$3.01 \times 10^{-10}$	$6.92 \times 10^{-8}$	$4.08 \times 10^{-8}$	$1.11 \times 10^{-7}$
POF [kg NMVOC eq]	$3.10 \times 10^{-5}$	$6.14 \times 10^{-5}$	$8.82 \times 10^{-3}$	$3.92 \times 10^{-3}$	$1.28 \times 10^{-2}$
RUF [MJ]	$1.26 \times 10^{-1}$	$2.98 \times 10^{-1}$	$4.82 \times 10^1$	$1.53 \times 10^1$	$6.39 \times 10^1$
RUm [kg Sb eq]	$2.92 \times 10^{-8}$	$5.10 \times 10^{-7}$	$3.76 \times 10^{-5}$	$6.14 \times 10^{-6}$	$4.42 \times 10^{-5}$
WU [m <sup>3</sup> depriv.]	$5.23 \times 10^{-4}$	$1.96 \times 10^{-2}$	2.18	$5.79 \times 10^{-1}$	2.78

The analysis covered energy sources for autoclave, heater, incubation, and scale consumption. The previously modelled Italian energy mix was replaced with energy from renewable sources, specifically from photovoltaic panels, modelled with the Ecoinvent dataset 'Electricity, low voltage {IT} electricity production, photovoltaic, 3kWp slanted-roof installation, multi-Si, panel, mounted | Cut-off, S'. The baseline scenario described above is referred to as S1 (Scenario 1), while the new scenario involving the use of photovoltaic panels is referred to as S2 (Scenario 2). Fig. 4 shows a comparison between the two scenarios, focusing on the contribution of energy consumption.

In fifteen of the sixteen impact categories considered, the use of energy from photovoltaic panels resulted in a lower impact, with reductions ranging from a maximum of 85% in categories such as IR, LU, and Ruf, to a minimum of 17% for the HTnc category. The only category showing an increase in impact is RUm: photovoltaic panels have a higher impact in terms of minerals and metals resource consumption, as their production requires specific raw materials, some of which are critical or rare earths elements. This impact is mainly attributable to the extraction and processing of these materials. The numerical data on the impacts are reported in SI, Table S8.

The LCA described above provides an initial overview of the potential impacts of the laboratory-scale process; however, when considering its application at an industrial scale, several significant complexities arise that may affect its overall sustainability. One key aspect is electricity consumption, which represents the largest contribution to environmental impact. If highly energy-intensive phases, such as incubation are scaled-up to industrial level, the transition could amplify the environmental footprint disproportionately compared to the increase in production capacity, as analyzed by Alaux *et al.*,<sup>42</sup> due to a non-linear rise in energy demand. Another critical factor to consider is the use of disposable equipment, whose volumes would become unsustainable at an industrial scale. This equipment should therefore be replaced with reusable alternatives, as without such a transition, the impacts

associated with plastic waste and its production would render the process difficult to sustain. In addition, it is essential to consider the availability and homogeneity of the materials composing the substrate, which must be ensured throughout the entire supply chain. Finally, when scaling to an industrial level, higher energy requirements and additional machinery may become necessary to replace laboratory operations that are performed manually with automated procedures, such as sample dosing and filling.<sup>44</sup> Scaling up does not necessarily imply an improvement in the sustainability of the process: while increased productivity and process optimization must certainly be considered, so too must the new environmental impacts arising from the energy consumption of additional processing stages, from transportation, from infrastructure, and from the management of equipment and laboratory materials.

### 3.6 Development of biocomposite prototypes

After confirming the effective degradation of the investigated compounds, each resulting material was thermally treated to deactivate fungal residues and subsequently assessed for its mechanical properties. All samples exhibited noticeable tactile brittleness: for this reason, they were deemed unsuitable for direct application. To enhance hardness, they were incorporated as fillers into a polymeric matrix. In accordance with sustainability goals and the principles of green chemistry, biodegradable and compostable materials, specifically polylactic acid and polyhydroxyalkanoates were selected. However, preliminary tests showed that these polymers were not suitable for encapsulating fungal substrates, as they became excessively brittle or demonstrated insufficient mechanical stability. PBAT was then tested as alternative polymeric matrix. Although PBAT has a fossil origin, it is fully biodegradable and compostable.<sup>45,46</sup> Using compounds containing a maximum 30% (w/w) of fungal substrate in PBAT matrix, previously mixed appropriately, helped avoid segregation issues that could compromise the extrusion of a uniform and continuous material. This



improvement can be explained by the different chemical and physical properties of PBAT and the fungal substrate: the lighter and cotton-like fungal powder tend to segregate if not properly broken down and dispersed, leading to inhomogeneous filaments.

The behavior of the produced specimens under tensile testing showed clear differences. ANOVA followed by a Bonferroni post hoc test confirmed statistically significant variations among samples ( $p < 0.05$ ). More specifically: (i) the Young's modulus (stiffness) increased significantly with higher fungal substrate content when compared to pure PBAT, indicating a stiffer material.<sup>47</sup> The fungal substrate acted as a structural filler, reinforcing the polymer matrix; (ii) yield stress (plasticity): no significant differences were observed among the formulations, indicating that incorporation of the fungal substrate did not substantially influence the transition from elastic to plastic deformation; (iii) maximum stress (stress at break): significant differences were observed between pure PBAT and all composite formulations, whereas no significant differences were found among the PBAT-fungal substrate mixtures. Pure PBAT exhibited the highest toughness. The reduced ability of the composites to withstand high stress before failure was likely due to weak interfacial adhesion, resulting in non-effective stress transfer between the filler and the polymer matrix. Therefore, these composites may be suitable for applications where enhanced rigidity is desired and high mechanical stresses are not expected, such as rigid secondary packaging or lightweight structural objects including combs or hairdressing bowls.

## 4 Conclusions

This study demonstrates the successful application of mixture design of experiments as an innovative and effective strategy to optimize fungal growth conditions for the bioremediation of cosmetic waste leveraging the properties of three WRF species. Reliable analytical method based on the green QuEChERS extraction technique and UHPLC-DAD enabled an accurate quantitation of dye degradation. The mixture design approach which exhibited high goodness of fit and predictive capability, demonstrating the crucial role of the substrate composition in influencing both fungal growth and final biocomposite consistency.

The optimization process produced an optimal mixture capable of increasing the waste-derived content from 37% to 60%, representing a substantial advancement in circular waste management practices. This work not only confirms the high potential of WRF in degrading complex cosmetic waste but also establishes a scalable, data-driven methodology for optimizing fungal-based bioprocesses.

The gate-to-gate LCA of the production process, conducted at a laboratory scale, revealed that energy consumption by the machinery, particularly during the incubation phase, was the step with the greatest environmental impact for 14 out of the 16 impact categories considered. Future work will focus on scaling up the process to an industrial level, allowing for a more

accurate assessment of the impacts associated with energy consumption.

The results achieved in this study are particularly noteworthy in the context of the circular economy, as they highlight the potential of sustainable practices not only to reduce waste, but also to add value through resource recovery and reuse. In the next future, the resulting fungal-based material will be used in the production of biodegradable and compostable secondary packaging material to close the circular loop and offer an environmentally friendly alternative to conventional plastic-based packaging solutions.

## Author contributions

Conceptualization: F. Bianchi, P. Goi; data curation: E. Ribeazzi, F. Fornari, N. Riboni, A. Mori, G. Vignali, C. Sciancalepore; formal analysis: E. Ribeazzi, F. Fornari, N. Riboni, M. Mattarozzi, A. Mori, M.V. Rizzo; methodology: P. Goi, F. Bianchi, M. Careri, C. Sciancalepore, G. Vignali; supervision: P. Goi, F. Bianchi, G. Vignali; visualization: E. Ribeazzi, F. Fornari, N. Riboni, M. Piergiovanni; writing original draft: E. Ribeazzi, F. Fornari, N. Riboni, M. V. Rizzo, F. Bianchi; writing-review and editing: N. Riboni, A. Mori, P. Goi, M. Mattarozzi, M. Piergiovanni, C. Sciancalepore, D. Milanese, G. Vignali, F. Bianchi, M. Careri. All authors have given approval to the final version of the manuscript.

## Conflicts of interest

There are no conflicts to declare.

## Data availability

The data supporting the findings of this study are available within the article and its supplementary information (SI). Additional data are available from the corresponding authors on reasonable request. Supplementary information: materials and reagents, optimization of fungal growth conditions, model regression, QuEChERS extraction, degradation experiments method validations, life cycle assessment, software used for the analysis, tables and figures. See DOI: <https://doi.org/10.1039/d5su00770d>.

## Acknowledgements

This work has benefited from the equipment and framework of the COMP-R Initiative, funded by the 'Departments of Excellence' program of the Italian Ministry for Education, University and Research (MUR, 2023–2027).

## References

- 1 Circular economy: definition, importance and benefits, <https://www.europarl.europa.eu/topics/en/article/20151201STO05603/circular-economy-definition-importance-and-benefit>.



2 S. Dey, F. Bano and A. Malik, in *Pharmaceuticals and Personal Care Products: Waste Management and Treatment Technology*, Elsevier, 2019, pp. 1–26.

3 S. Sungur, in *Emerging Contaminants in the Environment*, Elsevier, 2022, pp. 137–157.

4 S. Da França, M. Dario, V. Esteves, A. Baby and M. Velasco, Types of Hair Dye and Their Mechanisms of Action, *Cosmetics*, 2015, **2**, 110–126.

5 P. Ghosh and A. K. Sinha, Hair Colors: Classification, Chemistry and a Review of Chromatographic and Electrophoretic Methods for Analysis, *Anal. Lett.*, 2008, **41**, 2291–2321.

6 List of 181 substances banned for use in hair dye products, <https://ec.europa.eu/docsroom/documents/13209/attachments/1/translations>.

7 List of substances allowed for restricted use in hair dye products, <https://ec.europa.eu/docsroom/documents/22242>.

8 J. Deacon, *Fungal Biology*, Wiley, USA, 4th edn., 2005.

9 L. F. Longe, J. Couvreur, M. Leriche Grandchamp, G. Garnier, F. Allais and K. Saito, Importance of Mediators for Lignin Degradation by Fungal Laccase, *ACS Sustain. Chem. Eng.*, 2018, **6**, 10097–10107.

10 S. K. Sen, S. Raut, P. Bandyopadhyay and S. Raut, Fungal decolouration and degradation of azo dyes: A review, *Fungal Biol. Rev.*, 2016, **30**, 112–133.

11 A. C. Sousa, L. O. Martins and M. P. Robalo, Laccases: Versatile Biocatalysts for the Synthesis of Heterocyclic Cores, *Molecules*, 2021, **26**, 3719.

12 M. Tekere, A. Mswaka, R. Zvauya and J. Read, Growth, dye degradation and ligninolytic activity studies on Zimbabwean white rot fungi, *Enzyme Microb. Technol.*, 2001, **28**, 420–426.

13 A. Pandi, G. Marichetti Kuppuswami, K. Numbi Ramudu and S. Palanivel, A sustainable approach for degradation of leather dyes by a new fungal laccase, *J. Clean. Prod.*, 2019, **211**, 590–597.

14 B. Viswanath, B. Rajesh, A. Janardhan, A. P. Kumar and G. Narasimha, Fungal Laccases and Their Applications in Bioremediation, *Enzym. Res.*, 2014, **2014**, 1–21.

15 C. Girometta, A. M. Picco, R. M. Baiguera, D. Dondi, S. Babbini, M. Cartabia, M. Pellegrini and E. Savino, Physico-Mechanical and Thermodynamic Properties of Mycelium-Based Biocomposites: A Review, *Sustainability*, 2019, **11**, 281.

16 K. Joshi, M. K. Meher and K. M. Poluri, Fabrication and Characterization of Bioblocks from Agricultural Waste Using Fungal Mycelium for Renewable and Sustainable Applications, *ACS Appl. Bio Mater.*, 2020, **3**, 1884–1892.

17 A. Galuszka, Z. Migaszewski and J. Namieśnik, The 12 principles of green analytical chemistry and the SIGNIFICANCE mnemonic of green analytical practices, *TrAC, Trends Anal. Chem.*, 2013, **50**, 78–84.

18 Á. Santana-Mayor, B. Socas-Rodríguez, A. V. Herrera-Herrera and M. Á. Rodríguez-Delgado, Current trends in QuEChERS method. A versatile procedure for food, environmental and biological analysis, *TrAC, Trends Anal. Chem.*, 2019, **116**, 214–235.

19 *Eurachem Guide: the Fitness for Purpose of Analytical Methods – A Laboratory Guide to Method Validation and Related Topics*, ed. H. Cantwell, Eurachem Guid., 1998, pp. 1–61, ISBN 0-94948926-12-0.

20 International Organization for Standardization, *Environmental Management — Life Cycle Assessment: Principles and Framework*, ISO 14040, Geneva, 2006.

21 International Organization for Standardization, *Environmental Management — Life Cycle Assessment — Requirements and Guidelines*, ISO 14044, Geneva, 2006.

22 R. Zhuo and F. Fan, A comprehensive insight into the application of white rot fungi and their lignocellulolytic enzymes in the removal of organic pollutants, *Sci. Total Environ.*, 2021, **778**, 146132.

23 S. Rodríguez Couto and J. L. Toca Herrera, Industrial and biotechnological applications of laccases: A review, *Biotechnol. Adv.*, 2006, **24**, 500–513.

24 P. Baldrian, Fungal laccases – occurrence and properties, *FEMS Microbiol. Rev.*, 2006, **30**, 215–242.

25 Y. Chang, D. Yang, R. Li, T. Wang and Y. Zhu, Textile Dye Biodecolorization by Manganese Peroxidase: A Review, *Molecules*, 2021, **26**, 4403.

26 D. Linde, F. J. Ruiz-Dueñas, E. Fernández-Fueyo, V. Guallar, K. E. Hammel, R. Pogni and A. T. Martínez, Basidiomycete DyPs: Genomic diversity, structural-functional aspects, reaction mechanism and environmental significance, *Arch. Biochem. Biophys.*, 2015, **574**, 66–74.

27 V. D. Giap, H. T. Duc, P. T. M. Huong, D. T. Hanh, D. H. Nghi, V. D. Duy and D. T. Quynh, Purification and characterization of lignin peroxidase from white-rot fungi *Pleurotus pulmonarius* CPG6 and its application in decolorization of synthetic textile dyes, *J. Gen. Appl. Microbiol.*, 2022, **68**, 262–269.

28 V. Benavides, G. Ciudad, F. Pinto-Ibieta, T. Robledo, O. Rubilar and A. Serrano, Enhancing Laccase and Manganese Peroxidase Activity in White-Rot Fungi: The Role of Copper, Manganese, and Lignocellulosic Substrates, *Agronomy*, 2024, **14**, 2562.

29 E. Fernández-Fueyo, F. J. Ruiz-Dueñas, M. J. Martínez, A. Romero, K. E. Hammel, F. J. Medrano and A. T. Martínez, Ligninolytic peroxidase genes in the oyster mushroom genome: heterologous expression, molecular structure, catalytic and stability properties, and lignin-degrading ability, *Biotechnol. Biofuels*, 2014, **7**, 2.

30 J. Cuamatzi-Flores, S. Nava-Galicia, E. U. Esquivel-Naranjo, A. Lopez Munguia, A. Arroyo-Becerra, M. A. Villalobos-López and M. Bibbins-Martínez, Regulation of dye-decolorizing peroxidase gene expression in *Pleurotus ostreatus* grown on glycerol as the carbon source, *PeerJ*, 2024, **12**, 17467.

31 D. A. Johnnie, R. Issac, M. L. Prabha and L. A. Gomez, Biodegradation Assay of Heavy Metals and Dyes Decolorization in Textile Industrial Effluent using Laccase Isolated from *Pleurotus ostreatus*, *J. Pure Appl. Microbiol.*, 2023, **17**, 2324–2343.

32 H. El-Ramady, N. Abdalla, Z. Fawzy, K. Badgar, X. Llanaj, G. Törös, P. Hajdú, Y. Eid and J. Prokisch, Green



Biotechnology of Oyster Mushroom (*Pleurotus ostreatus* L.): A Sustainable Strategy for Myco-Remediation and Bio-Fermentation, *Sustainability*, 2022, **14**, 3667.

33 E. M. Ko, Y. E. Leem and H. T. Choi, Purification and characterization of laccase isozymes from the white-rot basidiomycete *Ganoderma lucidum*, *Appl. Microbiol. Biotechnol.*, 2001, **57**, 98–102.

34 P. Qin, Y. Wu, B. Adil, J. Wang, Y. Gu, X. Yu, K. Zhao, X. Zhang, M. Ma, Q. Chen, X. Chen, Z. Zhang and Q. Xiang, Optimization of Laccase from *Ganoderma lucidum* Decolorizing Remazol Brilliant Blue R and Glac1 as Main Laccase-Contributing Gene, *Molecules*, 2019, **24**, 3914.

35 F. Bianchi, M. Careri, A. Mangia, M. Mattarozzi and M. Musci, Experimental design for the optimization of the extraction conditions of polycyclic aromatic hydrocarbons in milk with a novel diethoxydiphenylsilane solid-phase microextraction fiber, *J. Chromatogr. A*, 2008, **1196–1197**, 41–45.

36 D. P. Di Lonardo, A. van der Wal, P. Harkes and W. de Boer, Effect of nitrogen on fungal growth efficiency, *Plant Biosyst.*, 2020, **154**, 433–437.

37 M. Anastassiades, S. J. Lehotay, D. Štajnbaher and F. J. Schenck, Fast and Easy Multiresidue Method Employing Acetonitrile Extraction/Partitioning and “Dispersive Solid-Phase Extraction” for the Determination of Pesticide Residues in Produce, *J. AOAC Int.*, 2003, **86**, 412–431.

38 AOAC 2007.01-2007, Pesticide residues in foods by acetonitrile, [http://www.aoacofficialmethod.org/index.php?main\\_page=product\\_info&products\\_id=2155](http://www.aoacofficialmethod.org/index.php?main_page=product_info&products_id=2155).

39 CSN EN 15662, Foods of plant origin - Multimethod for the determination of pesticide residues using GC- and LC-based analysis following acetonitrile extraction/partitioning and clean-up by dispersive SPE - Modular QuEChERS-method, <https://www.en-standard.eu/csn-en-15662-foods-of-plant-origin-multimethod-for-the-determination-of-pesticide-residues-using-gc-and-lc-based-analysis-following-acetonitrile-extraction-partitioning-and-clean-up-by-dispersive-spe-modular-quechers-method>.

40 W. Zhou, S. Yang and P. G. Wang, Matrix Effects and Application of Matrix Effect Factor, *Bioanalysis*, 2017, **9**, 1839–1844.

41 Welcome to LC - IMPACT, <https://www.lc-impact.eu>.

42 N. Alaux, H. Vašatko, D. Maierhofer, M. R. M. Saade, M. Stavric and A. Passer, Environmental potential of fungal insulation: a prospective life cycle assessment of mycelium-based composites, *Int. J. Life Cycle Assess.*, 2024, **29**, 255–272.

43 H. Bahua, S. P. Wijayanti, A. S. Putra, N. R. Ariyani, F. Isharyadi, N. Nuha, A. K. Paminto, M. Mulyono, I. N. Djarot, N. Widyastuti, A. I. Sitomurni, A. A. R. Setiawan and T. Handayani, Life cycle assessment (LCA) of leather-like materials from mycelium: Indonesian case study, *Int. J. Life Cycle Assess.*, 2024, **29**, 1916–1931.

44 L. Stelzer, F. Hoberg, V. Bach, B. Schmidt, S. Pfeiffer, V. Meyer and M. Finkbeiner, Life Cycle Assessment of Fungal-Based Composite Bricks, *Sustainability*, 2021, **13**, 11573.

45 C. Sciancalepore, E. Tigliatti, M. Marozzi, F. M. A. Rizzi, D. Pugliese, A. Cavazza, O. Pitirillo, M. Grimaldi and D. Milanese, Flexible PBAT-Based Composite Filaments for Tunable FDM 3D Printing, *ACS Appl. Bio Mater.*, 2022, **5**, 3219–3229.

46 E. Tigliatti, D. Milanese, D. Pugliese and C. Sciancalepore, Viscoelastic Characterization and Degradation Stability Investigation of Poly(butylene adipate-co-terephthalate) - Calcium-Phosphate Glass Composites, *J. Polym. Environ.*, 2022, **30**, 3914–3933.

47 C. Sciancalepore, E. Tigliatti, A. Giubilini, D. Pugliese, F. Moroni, M. Messori and D. Milanese, Preparation and characterization of innovative poly(butylene adipate terephthalate)-based biocomposites for agri-food packaging application, *J. Appl. Polym. Sci.*, 2022, **24**, 139.

